# Extensive Sugar Modification Improves Triple Helix Forming Oligonucleotide Activity in Vitro but Reduces Activity in Vivo†

Md. Rowshon Alam,‡ Alokes Majumdar,‡ Arun Kalliat Thazhathveetil,‡ Su-Ting Liu,‡ Ji-Lan Liu,‡ Nitin Puri,‡ Bernard Cuenoud,§ Shigeki Sasaki,|| Paul S. Miller,⊥ and Michael M. Seidman*,‡

*Laboratory of Molecular Gerontology, National Institute on Aging, National Institutes of Health, Baltimore, Maryland 21224, Novartis Pharmaceuticals Ltd., 4002 Basel, Switzerland, Graduate School of Pharmaceutical Sciences, Kyushu University, Fukuoka 812-8582, Japan, and Department of Biochemistry and Molecular Biology, Bloomberg School of Public Health, Johns Hopkins University, Baltimore, Maryland 21205*

*Received February 14, 2007; Revised Manuscript Received May 11, 2007*

ABSTRACT: We are developing triple helix forming oligonucleotides (TFOs) for gene targeting. Previously, we synthesized bioactive TFOs containing 2′-*O*-methylribose (2′-OMe) and 2′-*O*-aminoethylribose (2′-AE) residues. Active TFOs contained four contiguous 2′-AE residues and formed triplexes with high thermal stability and rapid association kinetics. In an effort to further improve bioactivity, we synthesized three series of TFOs containing the 2′-AE patch and additional ribose modifications distributed throughout the remainder of the oligonucleotide. These were either additional 2′-AE residues, the conformationally locked BNA/LNA ribose with a 2′-*O*,4′-*C*-methylene bridge, or the 2′-*O*,4′-*C*-ethylene analogue (ENA). The additionally modified TFOs formed triplexes with greater thermal stability than the reference TFO, and some had improved association kinetics. However, the most active TFOs in the biochemical and biophysical assays were the least active in the bioassay. We measured the thermal stability of triplexes formed by the TFOs in each series on duplex targets containing a change in sequence at a single position. The $T_m$ value of the variant sequence triplexes increased as the number of all additional modifications increased. A simple explanation for the failure of the improved TFOs in the bioassay was that the increased affinity for nonspecific targets lowered the effective nuclear concentration. Enhancement of TFO bioactivity will require chemical modifications that improve interaction with the specific targets while retaining selectivity against mismatched sequences.

A DNA triple helix consists of a third strand of nucleic acid of appropriate sequence bound in the major groove of an intact duplex (*1*). These structures form most readily in polypurine·polypyrimidine tracts and are stabilized by hydrogen bonds between the third strand bases and the duplex purines (*2*). Depending on the target sequence the TFO might consist of purines or pyrimidines. However, in both motifs the hydrogen-bonding interactions are sequence specific, and a triplex binding code has been elucidated (*3*) (reviewed in ref *4*). Although the focus of extensive biochemical and biophysical analyses (*5*), it has been appreciated for many years that TFOs might have application as reagents for gene targeting in living mammalian cells (*6*−*9*). While triplex formation is straightforward under controlled conditions in vitro, the nuclear environment of living cells presents substantial obstacles. The third strand oligonucleotide must be nuclease resistant, overcome the charge repulsion between the third strand phosphates and those of the duplex target, form a triplex in physiological pH, and surmount entropic barriers to formation of a structure imposing constraints on both members of the complex. Conventional deoxyoligonucleotides perform poorly in the face of these challenges.

Base and sugar modifications that address these issues have been described. For example, 5-methylcytosine, as a cytosine replacement, was shown many years ago to ameliorate the pH restrictions on TFOs in the pyrimidine motif (*10*). The observation that RNA third strands formed more stable triplexes than their deoxy counterparts (*11*) prompted the synthesis and characterization of TFOs containing a number of ribose analogues. 2′-Methoxylation (2′-OMe) (*12*, *13*) stabilizes the C3′-endo conformation of the sugar, which is optimal for triplex formation, and imposes the least distortion on the duplex target (*14*). The 2′-AE analogue combines the C3′-endo character with a positive charge, as the amine is protonated at physiological pH. This reduces the charge repulsion between the third strand and the duplex target, increases the association rate, and enhances triplex stability after formation (*15*−*17*). The C3′-endo conformation can be locked by bridging the 2′ and 4′ positions, as has been shown with two derivatives. TFOs with a 2′-*O*,4′-*C*-methylene linkage in some of the sugars (BNA/LNA) form triplexes with increased thermal stability and decreased dissociation rates (*18*−*20*). Similarly, incorporation of the 2′-*O*,4′-*C*-ethylene-bridged analogue (ENA) enhances triplex thermal

† The research described here was supported by the Intramural Research Program of the National Institute on Aging, National Institutes of Health.

* Corresponding author: phone, 410-558-8565; fax, 410-558-8157; e-mail, seidmanm@grc.nia.nih.gov.

‡ National Institute on Aging, NIH.

§ Novartis Pharmaceuticals Ltd.

|| Kyushu University.

⊥ Johns Hopkins University.

10.1021/bi7003153 CCC: $37.00 
Published on Web 08/11/2007

stability and extends third strand residence time (*21*). Neither of the locked sugar modifications improves association rate.

We are developing TFOs as gene targeting reagents for use in living cells. We established a quantitative assay of TFO bioactivity based on the targeted knockout of the *HPRT* gene, well-known as an endogenous mutation reporter gene (*22*). The gene contains a polypurine·polypyrimidine element adjacent to a 5′ TA step, which is a preferred site for reaction with psoralen, a photoactive DNA cross-linking agent and potent mutagen. We used this assay to evaluate the bioactivity of psoralen-linked TFOs (pso-TFO) containing various modifications. The most successful TFOs had 2′-OMe ribose in most positions and a patch of three to four contiguous 2′-AE residues (*23*). Biochemical and biophysical characterization demonstrated that TFOs with adjacent 2′-AE residues had a faster association rate than a TFO with the same number of distributed 2′-AE residues, although the $T_m$ values of triplexes formed by both TFOs were similar. A study of several active and inactive TFOs demonstrated that bioactivity correlated with association rate rather than the thermal stability of triplexes formed by the TFOs (*23*). Additional experiments led us to conclude that triplex stability in vivo was much lower than in vitro. In such an environment TFOs with faster association rates would be favored in the *HPRT* mutation assay, which reports target occupancy by the pso-TFO at the time of photoactivation.

The conclusions from these experiments suggested that improvements in TFO bioactivity might be realized by additional modification that would increase triplex stability and maintain or enhance association rate. As a test of this hypothesis, we have constructed a series of TFOs containing a patch of 2′-AE residues and, variously, additional 2′-AE, BNA/LNA, or ENA substitutions. In this report we describe our characterization of these TFOs and the influence on bioactivity of these modifications.

## MATERIALS AND METHODS

*Phosphoramidites and CPG Supports*. $N^4$-Formamido-5′-*O*-(4,4′-dimethoxytrityl)-5-methylcytidine 2′-*O*-methyl-3′-*O*-(β-cyanoethyl-*N*,*N*-diisopropyl)phosphoramidite, 5′-*O*-(4,4′-dimethoxytrityl)-5-methyluridine 2′-*O*-methyl-3′-*O*-(β-cyanoethyl-*N*,*N*-diisopropyl)phosphoramidite, 6-[4′-(hydroxymethyl)-4,5′,8-trimethylpsoralen]hexyl-1-*O*-(β-cyanoethyl-*N*,*N*-diisopropyl)phosphoramidite, and 5′-*O*-(4,4′-dimethoxytrityl)-5-methyluridine 2′-*O*-methyl-3′-*O*-succinamido-$N^6$-hexanamido-$N^3$-propyl-CPG (controlled pore glass) support were purchased from Chemgenes, Ashland, MA. Synthesis of $N^4$-(*N*-methylpyrrolidinoamidino)-5′-*O*-(4,4′-dimethoxytrityl)-5-methylcytidine 2′-*O*-(2-aminoethyl)-3′-*O*-(β-cyanoethyl-*N*,*N*-diisopropyl)phosphoramidite and 5′-*O*-(4,4′-dimethoxytrityl)-5-methyluridine 2′-*O*-(2-aminoethyl)-3′-*O*-(β-cyanoethyl-*N*,*N*-diisopropyl)phosphoramidite was reported previously (*15*, *24*). 5′-*O*-(4,4′-Dimethoxytrityl)-5-methyluridine (2′-*O*,4′-*C*-methylene)-3′-[(2-cyanoethyl)(*N*,*N*-diisopropyl)]phosphoramidite was purchased from Glen Research, Sterling, VA. 5′-*O*-(4,4′-Dimethoxytrityl)-5-methyluridine (2′-*O*,4′-*C*-ethylene)-3′-*O*-[(2-cyanoethyl)(*N*,*N*-diisopropyl)]phosphoramidite and 5′-*O*-(4,4′-dimethoxytrityl)-2′-*O*,4′-*C*-ethylene-4-*N*-benzoyl-5-methylcytidine 3′-*O*-[(2-cyanoethyl)(*N*,*N*-diisopropyl)]-phosphoramidite (*25*) were purchased from Sankyo Lifetech Co., Ltd. (Tokyo, Japan).

*Synthesis, Deprotection, Purification, and Mass Determination of TFOs.* The oligonucleotides were synthesized on a 0.2 μmol scale on CPG supports (500 Å) using an Expedite 8909 synthesizer as previously described (*26*). The phosphoramidites were dissolved at a concentration of 0.1 M. The coupling times for the phosphoramidite monomers of protected 2′-*O*-methylthymidine and 2′-*O*-methyl-5-methylcytidine were 360 s. The coupling times for the phosphoramidite monomers of protected 2′-aminoethylthymidine, 2′-aminoethyl-5-methylcytidine, 2′-*O*,4′-*C*-BNA/LNA or ENA monomer, and psoralen were 900 s. The TFOs were deprotected with equal ratios (1:1) of 0.5 mL of 28% aqueous $NH_3$ and 0.5 mL of 40% aqueous methylamine (Aldrich Chemicals) solution for 90 min at room temperature, immediately evaporated to dryness, and resuspended in HPLC grade $H_2O$. Purification of TFOs was carried out by an ion-exchange HPLC using a Dionex DNAPac PA-100 column (column sizes are 4.0 mm × 250 mm for analysis and 9.0 mm × 250 mm for purification, respectively) on a Shimadzu HPLC system (LC-10ADvp) with a dual wavelength detector (SPD-10AVvp) and an autoinjector (SIL-10ADvp). HPLC conditions were as follows: linear gradient, % buffer B = 0−50% for 45 min, ∼100% for 60 min, 1.5 mL/min; buffer A consisted of 100 mM Tris (pH 7.8) containing 10% $CH_3CN$; buffer B consisted of 1 M NaCl containing 100 mM Tris (pH 7.8) and 10% $CH_3CN$; UV monitor, 254 and 315 nm ($\lambda_{max}$ for psoralen). The oligonucleotides were collected, lyophilized, and desalted using a Sep-Pak Plus C18 cartridge (Waters Corp.). The masses of the chemically modified oligonucleotides were determined by the positive ion mode using MALDI-TOF (matrix-assisted laser desorption ionization time of flight) mass spectroscopy on a Voyager Applied Biosystem Instrument. The matrix used for preparing the MALDI-TOF samples is a mixture of 3-hydroxypicolinic acid (50 mg $mL^{-1}$ in 50% $CH_3CN$) and ammonium citrate (50 mg $mL^{-1}$ in HPLC grade water). Analysis: AE-07, calculated 6151.37, found 6150.97; AE-AT-1, calculated 6177.34, found 6178.72; AE-AT-2, calculated 6206.36, found 6207.52; AE-AT-3, calculated 6235.38, found 6237.83; AE-AT-4, calculated 6264.40, found 6265.42; AE-BNA/LNA-1, calculated 6146.30, found 6147.79; AE-BNA/LNA-2, calculated 6144.28, found 6144.24; AE-BNA/LNA-3, calculated 6142.12, found 6140.90; AE-BNA/LNA-4, calculated 6140.24, found 6140.77; AE-ENA-1, calculated 6160.32, found 6162.78; AE-ENA-2, calculated 6172.32, found 6175.95; AE-ENA-3, calculated 6184.32, found 6186.28; AE-ENA-4, calculated 6196.32, found 6199.58; AE-ENA-3b, calculated 6184.32, found 6186.58. The accuracy of the mass measurement was ±0.05%.

*Thermal Denaturation.* The thermal melting experiments were carried out using TFOs with a 19-mer *HPRT* hamster duplex target (5′-GTAGAAGAAAAAAGAGAAA and 3′-CATCTTCTTTTTTCTCTTT) which had a $T_m$ value of 53.5 °C. A 1 μM stock solution of target duplex was prepared in a buffer containing 100 mM NaCl, 2 mM $MgCl_2$, and 10 mM sodium cacodylate at pH 7.0. The solution was heated to 80 °C for 15 min, allowed to reach room temperature over 4 h, and then stored in the refrigerator at 4 °C. An aliquot of TFO solution (1 μM) was added to 1 mL of the stock duplex at room temperature, and the mixture was incubated at room temperature overnight. Thermal melting determinations were carried out using a Cary 3E UV−vis spectropho-

tometer fitted with a thermostat sample holder and a temperature controller. The triplex solution was heated from 25 to 85 °C at a rate of 0.4 °C/min, and the absorbance at 260 nm was recorded as a function of the temperature. The raw data were processed using Sigma plot 5.0 software to determine the first derivative curve, from which the $T_m$ value was obtained. All analyses were performed at least twice with an error of no more than 0.5 °C. The thermal stability analysis for TFOs with the hairpin duplexes was performed similarly as above in the same buffer. However, in this case the triplex solution was heated from 37 to 90 °C at a rate of 0.4 °C/min, and the absorbance at 260 nm was recorded as a function of the temperature.

*Association Rate Analysis*. The TFO + duplex → triplex transition is accompanied by a decrease in UV absorbance. This decay curve has been exploited for estimating TFO association rates with the target duplex (*27*, *28*). To measure the association rate kinetics of TFOs, we used a 19-mer linear duplex target (5′-GTAGAAGAAAAAAGAGAAA and 3′-CATCTTCTTTTTTCTCTTT). A stock duplex solution was prepared in a kinetic buffer containing 150 mM KCl, 1 mM $MgCl_2$, and 10 mM sodium cacodylate at pH 7.2. Each strand concentration used was 1 $\mu$M. One milliliter of the duplex stock solution was monitored by UV (260 nm) in a cuvette at 25 °C, and it gave a horizontal line as a function of time. An aliquot of the TFO solution (1 $\mu$M) was added with vigorous mixing to 1 mL of the duplex stock solution. The mixing process was no longer than 10 s. The experiments were carried out on a Cary dual-beam spectrophotometer fitted with a Peltier temperature controller at 25 °C. The UV decay curves were fitted to second-order kinetics using software supplied with the instrument, where association rate constants were obtained. The rate constants reported here were taken from an average of three individual experiments.

*Polyacrylamide Gel Electrophoresis*. Five picomoles of the purine strand (5′-GTAGAAGAAAAAAGAGAAA) was $^{32}$P-end labeled using [$\gamma$-$^{32}$P]ATP (NEN) and T4 polynucleotide kinase (New England Biolabs, Beverly, MA) and annealed with 25 pmol of the pyrimidine strand (3′-CATCTTCTTTTTTCTCTTT). Then the $^{32}$P-end labeled duplex was diluted 100-fold with 2× triplex buffer (40 mM Tris, 20 mM $MgCl_2$, pH 7.0) to make a stock duplex solution. Ten microliters of stock duplex oligos was incubated with 10 $\mu$L of each TFO (4 $\mu$M stock in water) at room temperature overnight. The final concentrations of both duplex strands were negligible relative to the third strand concentration. For denaturing gel electrophoresis, the triplex mixtures were UVA treated (1.8 J/cm$^2$) for 5 min at 365 nm. Three microliters of loading dye (0.1% xylene cyanol, 0.1% bromophenol blue, and 95% formamide) was added to each of the triplex mixtures and heated to 90 °C for 5 min. The mixtures were loaded onto a 12% polyacrylamide gel containing 7 M urea in 1× TBE buffer and run for 2.5 h at 250 V. For native gel electrophoresis, the dye (0.1% xylene cyanol, 0.1% bromophenol blue, 5 $\mu$L) was added to each of the triplex mixtures, and the mixtures were immediately loaded onto a 12% polyacrylamide gel in 1× TAE buffer and run for 4 h at 150 V. Gels were visualized using a Fuji Phosphorimager and quantified using ImageQuant software.

*HPRT Knockout Assay*. Chinese hamster ovary (CHO) AA8 cells were grown in Dulbecco's modified Eagle medium (DMEM; Life Technologies), supplemented with 10% fetal calf serum (FBS), penicillin, streptomycin, and glutamine. Prior to an experiment, cells were cultured in HAT medium ($10^{-4}$ M hypoxanthine, $5 \times 10^{-6}$ M aminopterin, and $10^{-5}$ M thymine) for 1 week to eliminate preexisting *HPRT*-deficient cells. Briefly, cells were plated at subconfluent levels, and the next day the medium was changed to DMEM with 2% FBS and 2% DMSO. After 48 h, the cells were washed and incubated with complete medium containing 100 $\mu$M mimosine for 16 h to block them in the early S phase (~90% early S cells) (*29*). After 16 h, the cells were released from the mimosine block by feeding with DMEM and 10% FBS and further incubated for 4 h. In previous work, we have shown that the *HPRT* target is most accessible in cells in the mid-S phase (*30*). Consequently, all bioactivity assays were carried out with mid-S phase cells.

*TFO Delivery, Psoralen Treatment, and HPRT Mutation Assay*. Mid-S phase cells were mixed with TFOs at 4 $\mu$M. The TFOs were delivered into the cells by electroporation (Bio-Rad; 130 V, 960 $\mu$F). The electroporated cells were incubated at room temperature for 3 h and exposed to UVA light in a Rayonet chamber for 3 min at 1.8 J/cm$^2$. The cells were plated in complete medium for 8−10 days with two or three passages and then placed in a selective medium depleted of hypoxanthine and containing 20 $\mu$M thioguanine (200000 cells/100 mm dish). *HPRT*-defective cells survive in 6-thioguanine. Cells were also plated in selective medium without thioguanine to determine plating efficiency. After 10 days, thioguanine- (TG-) resistant colonies were counted.

## RESULTS

The triplex target sequence is found in intron 4, adjacent to exon 5, of the *hprt* gene in Chinese hamster ovary (CHO) cells. It consists of an uninterrupted 17 nt polypurine·polypyrimidine element terminating in a 5′ TA step, which can be efficiently cross-linked by psoralen (Figure 1a). The sequence of the third strand, linked to psoralen, is also shown. The structures of the modified nucleosides incorporated into the oligonucleotides described in this study are presented in Figure 1b.

*TFOs with Isolated AE Residues in Addition to an AE Cluster*. In our earlier work we found that TFOs with separated 2′-AE residues had poor activity in the *HPRT* knockout assay (*23*), while clustered 2′-AE residues were important for TFO bioactivity (*23*, *31*). Thus TFO AE-07 with a patch of four 2′-AE residues located at the 3′ end of the molecule has received the most frequent use in our biological experiments (*30*, *32*). In an effort to extend these observations and improve TFO activity, we examined the effect of adding 2′-AE residues to the AE-07 format (Figure 2a). The additional 2′-AE modifications were placed away from the patch and separated from one another so as to be consistent with the TFOs containing BNA/LNA residues (see below), which must be separated (*19*). Thermal stability analyses showed that these TFOs formed triplexes that were more stable than the AE-07 triplex ($T_m$ = 63.5 °C). The AE-AT-4 triplex had a $T_m$ value that was approximately 10 °C higher (73 °C) (Figure 2b). It should be noted that all thermal stability measurements discussed in this report were performed at pH 7.0, since our interest was in the development of bioactive TFOs. Analyses of the association rate indicated

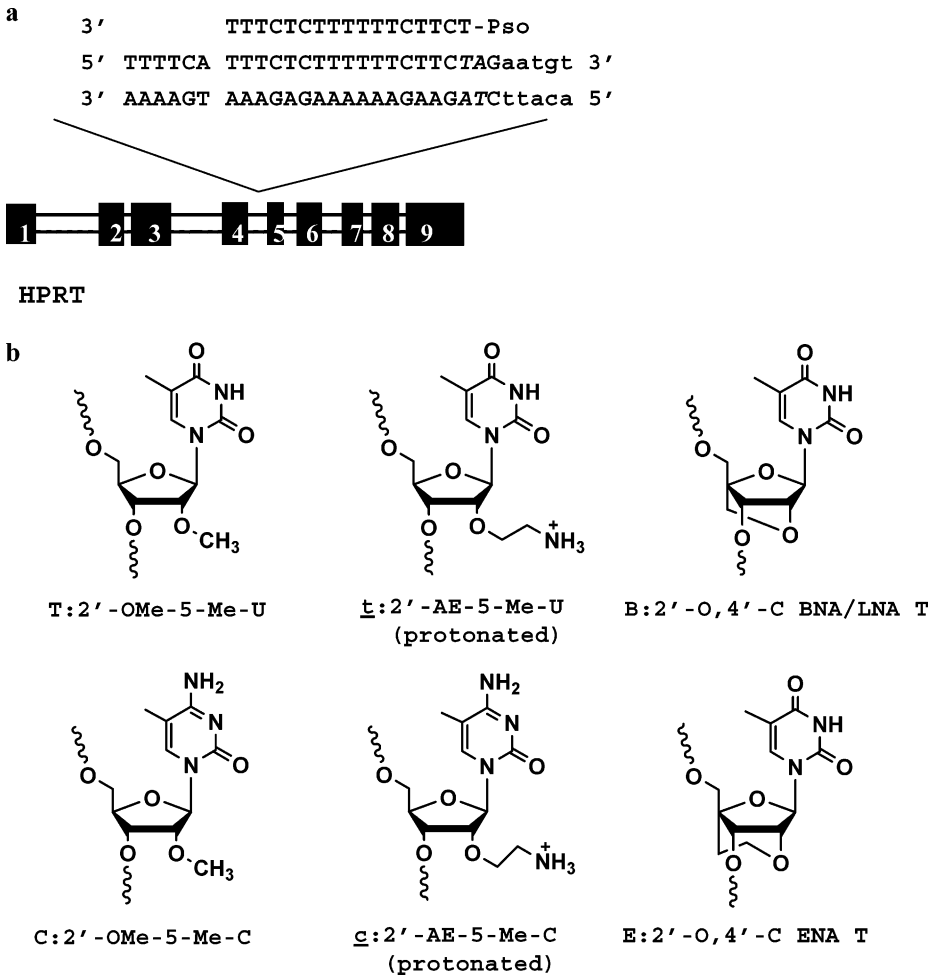


FIGURE 1: (a) The triplex target sequence in the Chinese hamster *HPRT* gene. The target lies in intron 4 adjacent to exon 5 (shown in lower case letters). The psoralen cross-link site 5′-TA step is shown in italics. The sequence and polarity of a TFO linked to psoralen are shown above the target sequence. (b) Structure of 2′-AE, 2′-OMe, and 2′-O,4′-C BNA/LNA (B) or ENA (E) nucleosides.

that the AE-AT TFOs had $k_{ON}$ values equivalent to or marginally greater than AE-07 (Figure 2c). These results demonstrated that the additional, isolated, 2′-AE residues improved the performance of the TFOs.

*Electrophoretic Analyses of Triplexes.* The triplexes formed by the AE-AT TFOs were examined by neutral gel electrophoresis. The band shift analysis indicated complete conversion of the labeled duplex to triplex by each TFO (Figure 3a). We then examined the integrity of the psoralen, a key element in our assay of TFO bioactivity. Psoralen is alkali labile, and the TFOs cannot be deprotected using standard procedures (Materials and Methods). We routinely test the activity of the psoralen by electrophoresis of the triplexes on a denaturing gel following photoactivation. Cross-linking connects the third strand and both strands of the duplex, and the three-stranded complex migrates in a denaturing gel more slowly than the individual single strands or a cross-linked duplex (which migrates just behind the single strand). As expected, this analysis showed that cross-linked triplexes formed by AE-07 had much slower mobility than the single strand marker. However, as a function of the additional 2′-AE content in the third strand, the complexes moved more rapidly, although not as rapidly as the labeled single strand from the denatured duplex (Figure 3b). This was particularly pronounced for the triplexes formed by AE-AT- 3 and AE-AT-4 (lanes 1 and 2). These results indicated that the TFOs with three and four additional 2′-AE residues formed triplexes that migrated in 7 M urea as structures that were more compact than the triplexes formed by the less extensively substituted TFOs.

*Biological Activity of the AE-AT TFOs*. The preceding results indicated that the TFOs with additional 2′-AE substitutions were able to form triplexes with superior stability and modestly enhanced association rates relative to the AE-07 TFO. On the basis of our previous experience we anticipated that these TFOs would be at least as effective, or perhaps more active, in the bioassay, as AE-07. The pso-AE-AT TFOs were electroporated into cells synchronized in the S phase, since our previous work demonstrated the greatest target access at this time (*30*). Following photoactivation of the psoralen the cells were processed through a standard thioguanine resistance assay to score mutagenesis of the *HPRT* target. In contrast to our expectation, we found that the bioactivity declined as a function of the additional AE content. The most effective TFO in the biochemical and biophysical assays (AE-AT-4) was the least active in the biological assay (Figure 4).

In previous work we have shown that the pso-TFO-targeted mutations reported by the *HPRT* mutation assays are deletions that inactivate the gene (*30*). Base substitutions are also formed at the target site, but these occur most frequently at a position that does not influence *HPRT* activity.

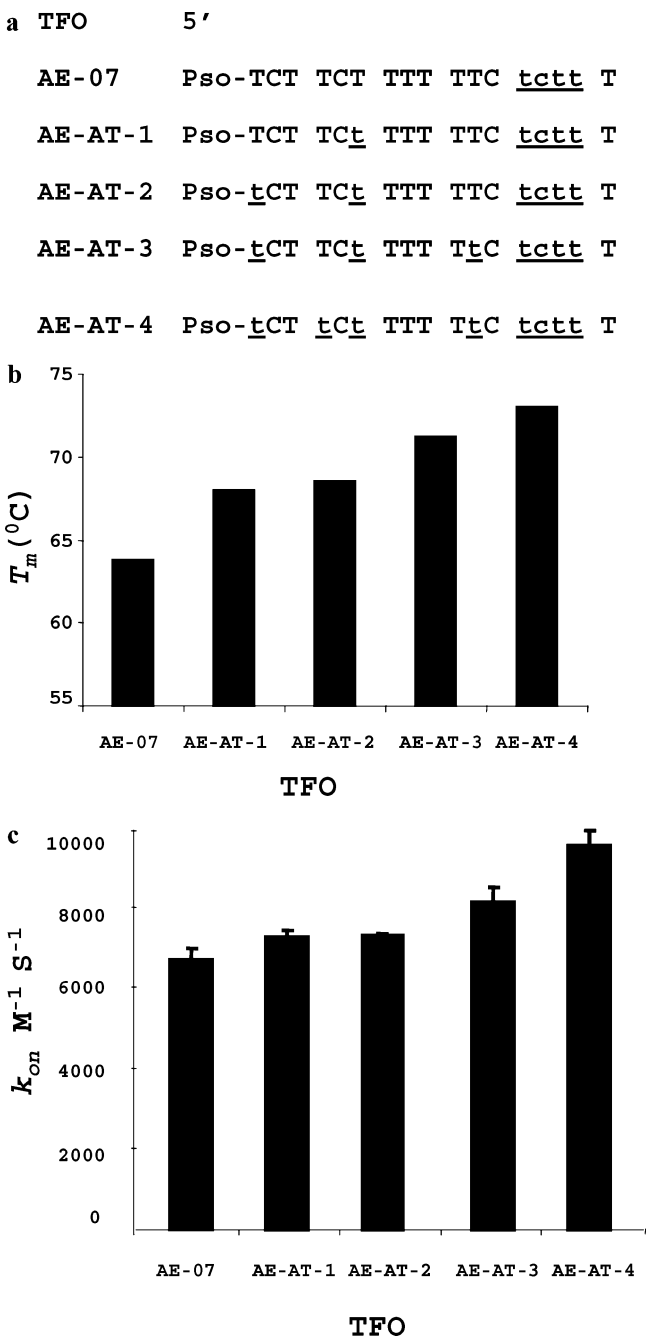


FIGURE 2: (a) Sequences and modification pattern of AE-07, AE-AT-1, -2, -3, and -4 TFOs. Each TFO contained four clustered 2′-AE residues (shown as tctt). AE-AT-1, -2, -3, and -4 contained one, two, three, and four additional, isolated 2′-AE residues (t), respectively. All TFOs were linked to psoralen at the 5′-end. (b) Thermal stability analysis ($T_m$) of triplexes formed by 2′-AE TFOs. (c) Relative association rate vs 2′-AE content.

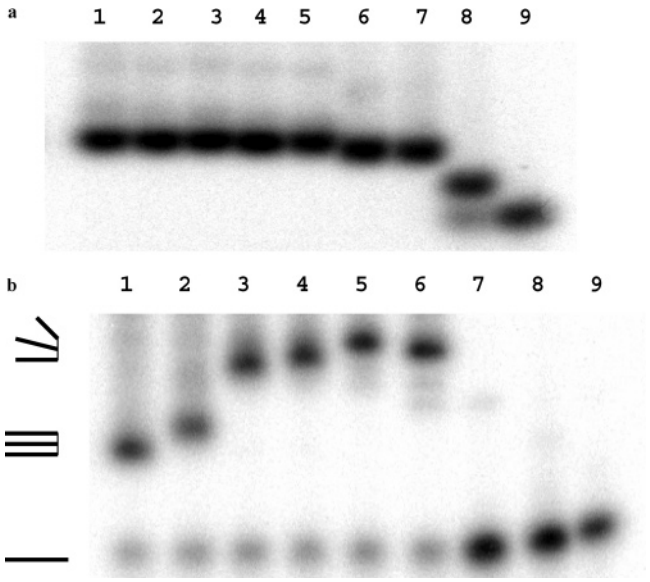


FIGURE 3: 12% polyacrylamide gel electrophoresis of triplexes: (a) nondenaturing and (b) denaturing conditions following cross-linking. The purine strand of the duplex was $^{32}P$ labeled. Lanes: 1, AE-AT-4 + duplex; 2, AE-AT-3 + duplex; 3, AE-AT-2 + duplex; 4, AE-AT-1 + duplex; 5, AE-07 + duplex; 6 and 7, Ps-4 + duplex; 8, duplex alone; 9, duplex purine strand. Lanes 1−6: The triplexes were UVA treated for 5 min to activate the psoralen prior to loading. The stick figures illustrate our interpretation of the structures in the bands.

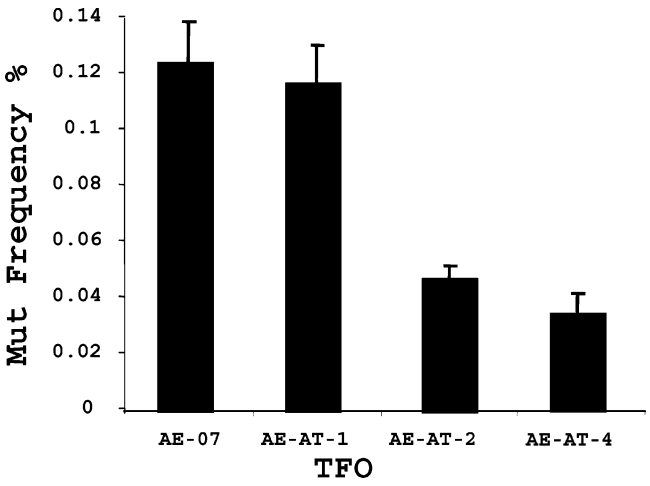


FIGURE 4: Bioactivity of AE-TFOs measured in the *HPRT* mutation assay.

Mutations at this site are silent in the *HPRT* assay. Consequently, we considered the possibility that the apparent decline in bioactivity of AE-AT-4 was due to a shift in the distribution between base substitution and deletion mutations. However, when we measured the base substitution frequency in cells treated with AE-AT-4, we found that it was lower as well (not shown). Thus AE-AT-4 was less effective by both measures of targeted mutagenesis.

*TFOs with BNA/LNA Substitutions.* One explanation for the decline in bioactivity of the AE-AT TFOs was that the added positive charge was counterproductive in vivo, perhaps because the TFOs were more adherent to proteins, membranes, etc. If bioavailability were a confounding variable, then AE-AT TFOs would not have been a legitimate test of our hypothesis that TFOs with enhanced performance in biochemical and biophysical assays would have improved activity in the biological assay. Consequently, we decided to examine substitutions that improved TFOs without adding positive charge. The BNA/LNA modification has been shown to enhance triplex stability (*18*, *33*), and the biophysical and biological properties of BNA/LNA TFOs have been characterized in considerable detail (*19*, *20*, *34*, *35*).

We first constructed a series of psoralen-linked oligonucleotides, containing 2′-OMe and one to four BNA/LNA residues (Figure 5a). The distribution of BNA/LNA residues was based on the pattern of 2′-AE substitution, outside the 2′-AE patch, in the AE-AT TFOs. This distribution also

followed the example of previous work that described the necessity of separating BNA/LNA residues in TFOs (*19*, *34*). As expected, these formed triplexes with $T_m$ values greater than those with only 2′-OMe modification. For example, the $T_m$ value of the triplex formed by the 2′-OMe TFO was 54.5 °C, while that of the mixed TFO with four BNA/LNA (BNA/LNA-4) was 73 °C. However, despite the enhancement in triplex stability that followed the introduction of the BNA/LNA residues, the BNA/LNA pso-TFOs were completely inactive in the *HPRT* bioassay (not shown).

We then synthesized pso-TFOs containing the 2′-AE cluster, with substitution of one to four 2′-OMeT by BNA/LNA T residues (Figure 5a). The thermal stability analysis showed a progressive increase in $T_m$ value as the BNA/LNA content increased. The $T_m$ value of the most extensively substituted TFO, AE-BNA/LNA-4 was 76.6 °C, a few degrees higher than the AE-AT4 triplex (Figure 5b). The association rate analysis indicated that there was a slight increase in association rate with the TFOs with two or three BNA/LNA substitutions. The TFO with four residues showed a decline, although still within the range of bioactive TFOs described by us previously (*36*) (Figure 5c). A duplex/triplex band shift experiment showed that all TFOs made stable triplexes as monitored by electrophoresis in a neutral acrylamide gel (not shown). Following photoactivation the triplexes were examined by electrophoresis in denaturing acrylamide gel. The results were strikingly similar to those with the AE-AT TFOs. The triplexes formed by the TFOs with zero, one, or two BNA/LNA modifications showed similar migration in 7 M urea. However, AE-BNA/LNA-3 and -4 triplexes displayed more rapid mobilities, much like the AE-AT-3 and AE-AT-4 triplexes (lanes 1 and 2, Figure 5d). As in the previous analyses, we concluded that triplexes formed by these two TFOs were able to maintain a more compact conformation in the denaturant than those formed by less extensively substituted oligonucleotides.

The AE-BNA/LNA-3 and AE-BNA/LNA-4 TFOs were then examined in the *HPRT* bioassay. Again, we found an inverse correlation with $T_m$ value and bioactivity (Figure 5e). The AE-BNA/LNA-4 TFO was completely inactive, while AE-BNA/LNA-3 had about 10% the activity of the reference TFO, AE-07.

*TFOs with ENA Substitutions.* BNA/LNA substitutions have been associated with oligonucleotide aggregation (*19*), and attention has been drawn to the pronounced conformational consequences of the BNA/LNA substitutions (*34*). Both features might compromise performance in vivo and reduce activity in the bioassay. The 2′-*O*,4′-*C*-ethylene-(ENA-) bridged ribose is also fixed in the C3′-endo conformation but is more flexible (*21*). Oligonucleotides with ENA substitutions also have the advantage of greater nuclease resistance than their BNA/LNA counterparts (*37*). TFOs containing the AE cluster and ENA-T residues arranged as in the previous experiments were synthesized (Figure 6a). The TFOs were characterized, as above, by thermal stability analysis. The $T_m$ values increased as the ENA content increased, in keeping with the previous series of TFOs (Figure 6b). In contrast to the AE-AT and the AE-BNA/LNA-1−3 TFOs, the association rate determination indicated that the ENA TFOs had $k_{ON}$ values that declined relative to AE-07 (Figure 6c). However, this appeared to reflect that placement of the ENA residues, as AE-ENA-3b, with a different arrangement of ENA substitutions showed an increase in association rate relative to AE-07. The analysis of the psoralen cross-linked triplexes by electrophoresis on a denaturing acrylamide gel again showed the faster mobility of the triplexes formed by the more extensively substituted TFOs (lanes 1, 2, and 3, Figure 6d). We then measured the bioactivity of the AE-ENA-3 and -3b TFOs. The results were similar to those found with the previous series of TFOs: there was a sharp reduction in activity with AE-ENA-3b (15% of AE-07) and no activity with AE-ENA-3 (Figure 6e).

*Thermal Stability of Triplexes Formed by TFOs on Variant Sequence Targets.* The strikingly similar results with the three different groups of TFOs argued that the additional sugar modifications, despite the apparent improvement in the biochemical and biophysical performance, were counterproductive in terms of bioactivity. Although there are a variety of candidate explanations, one of the simplest is that the increase in triplex stability against the specific target sequence was accompanied by a corresponding increase in stability of triplexes formed on nonspecific targets. A genome filled with nonspecific target sequences might sequester high-affinity TFOs, thus reducing their activity against the specific target. This argument is based on the assumption that the intranuclear TFO concentration following electroporation is not saturating for specific and nonspecific binding. In previous work we have shown a linear dependence of gene targeting activity on the dose of TFO used in the electroporation chamber in the concentration range employed in these experiments (*32*). Those results indicate that the intranuclear TFO concentration is not saturating and thus support the possibility that nonspecific binding could lower TFO concentration.

To characterize the affinity of the TFOs for nonspecific targets, we measured the thermal stability of triplexes formed by the TFOs on four hairpin duplex targets. One duplex contained the wild-type sequence while the others had a single alteration in sequence: a C·G, T·A, or G·C replacement of the same A·T pair (Figure 7a). The hairpin duplexes, which had $T_m$ values of approximately 75 °C, were used to eliminate the contribution of duplex melting to hyperchromic shifts that might occur in the range of 50−60 °C. Each TFO formed triplexes on the variant target duplexes. The thermal stability of the variant triplexes rose as the additional AE, BNA/LNA, or ENA content increased, just as with the perfectly matched triplexes. However, there was a distinction between the AE-AT series and the AE-BNA/LNA and AE-ENA series. The differential in $T_m$ value between the triplexes on the perfect and variant targets was largely maintained within the AE-AT series. Thus there was a 21.3 °C $T_m$ value difference between the triplexes formed by AE-07 on the perfectly matched target and the C·G-substituted variant target. Similarly, the difference between the corresponding AE-AT-4 triplexes was 19.6 °C (Figure 7b). Even with the more stable G·C variant triplexes a 10−12 °C differential was maintained. This differential narrowed with the TFOs with more extensive BNA/LNA and AE-ENA substitutions, particularly with the G·C variant (Figure 7c,d).

Despite these differences between the different TFO families, the results clearly indicated that an increase in affinity for a mismatched target accompanied the increased stability of triplexes formed by the extensively modified TFOs on the specific target. Note that the $T_m$ values of the

a

| TFO | 5′ |
|---|---|
| Ps-4 | Pso-TCT TCT TTT TTC TCT TT |
| BNA/LNA-1 | Pso-TCT TCB TTT TTC TCT TT |
| BNA/LNA-2 | Pso-BCT TCB TTT TTC TCT TT |
| BNA/LNA-3 | Pso-BCT TCB TTT TBC TCT TT |
| BNA/LNA-4 | Pso-BCT BCB TTT TBC TCT TT |
| AE-BNA/LNA-1 | Pso-TCT TCB TTT TTC tctt T |
| AE-BNA/LNA-2 | Pso-BCT TCB TTT TTC tctt T |
| AE-BNA/LNA-3 | Pso-BCT TCB TTT TBC tctt T |
| AE-BNA/LNA-4 | Pso-BCT BCB TTT TBC tctt T |

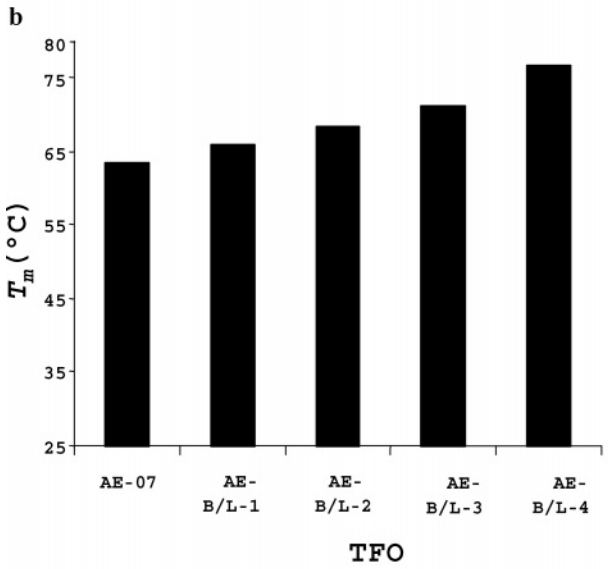


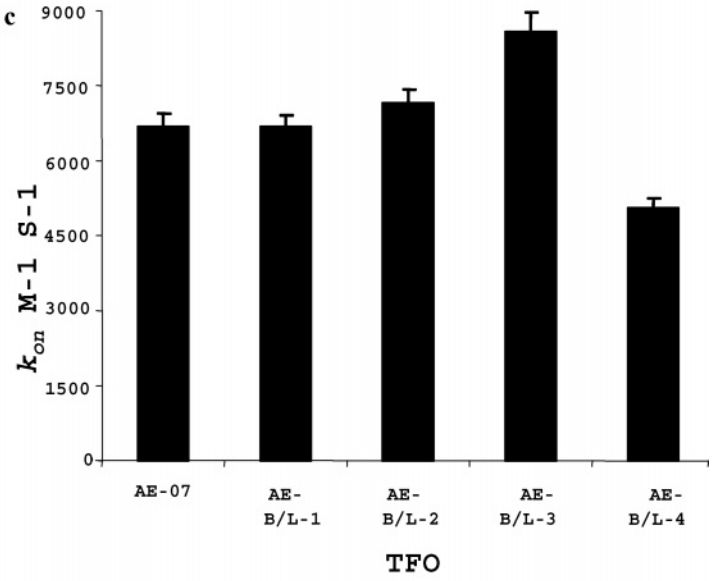


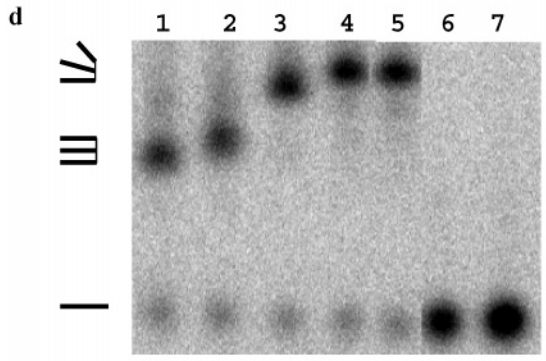


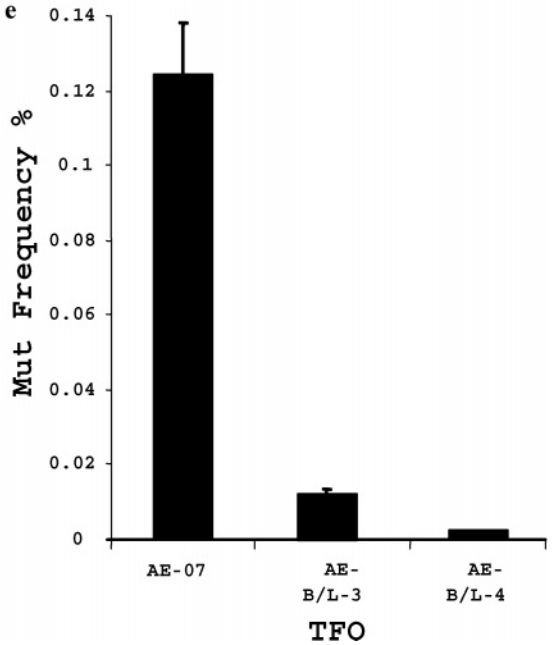


FIGURE 5: (a) Sequences and modification pattern of BNA/LNA TFOs and a parent TFO, Ps-4. B indicates 2′-O,4′-C BNA/LNA thymidine. BNA/LNA-1, -2, -3, and -4 contained one, two, three, and four B residues, respectively. The corresponding AE-TFOs contained four clustered 2′-AE residues (tctt). All TFOs contained psoralen at the 5′ end. (b) Thermal stability analysis of triplexes formed by AE-BNA/LNA TFOs. (c) Relative association rate vs BNA/LNA content. (d) Electrophoretic mobility of cross-linked triplexes on a denaturing 12% polyacrylamide gel. Extraneous lanes were removed from the gel profile. Lanes: 1, AE-BNA/LNA-4 + duplex; 2, AE-BNA/LNA-3 + duplex; 3, AE-BNA/LNA-2 + duplex; 4, AE-BNA/LNA-1 + duplex; 5, AE-07 + duplex; 6, duplex alone; 7, duplex purine strand. Lanes 1−5: The triplexes were UVA treated for 5 min prior to loading. (e) Bioactivity of AE-BNA/LNA TFOs measured in the *HPRT* mutation assay.

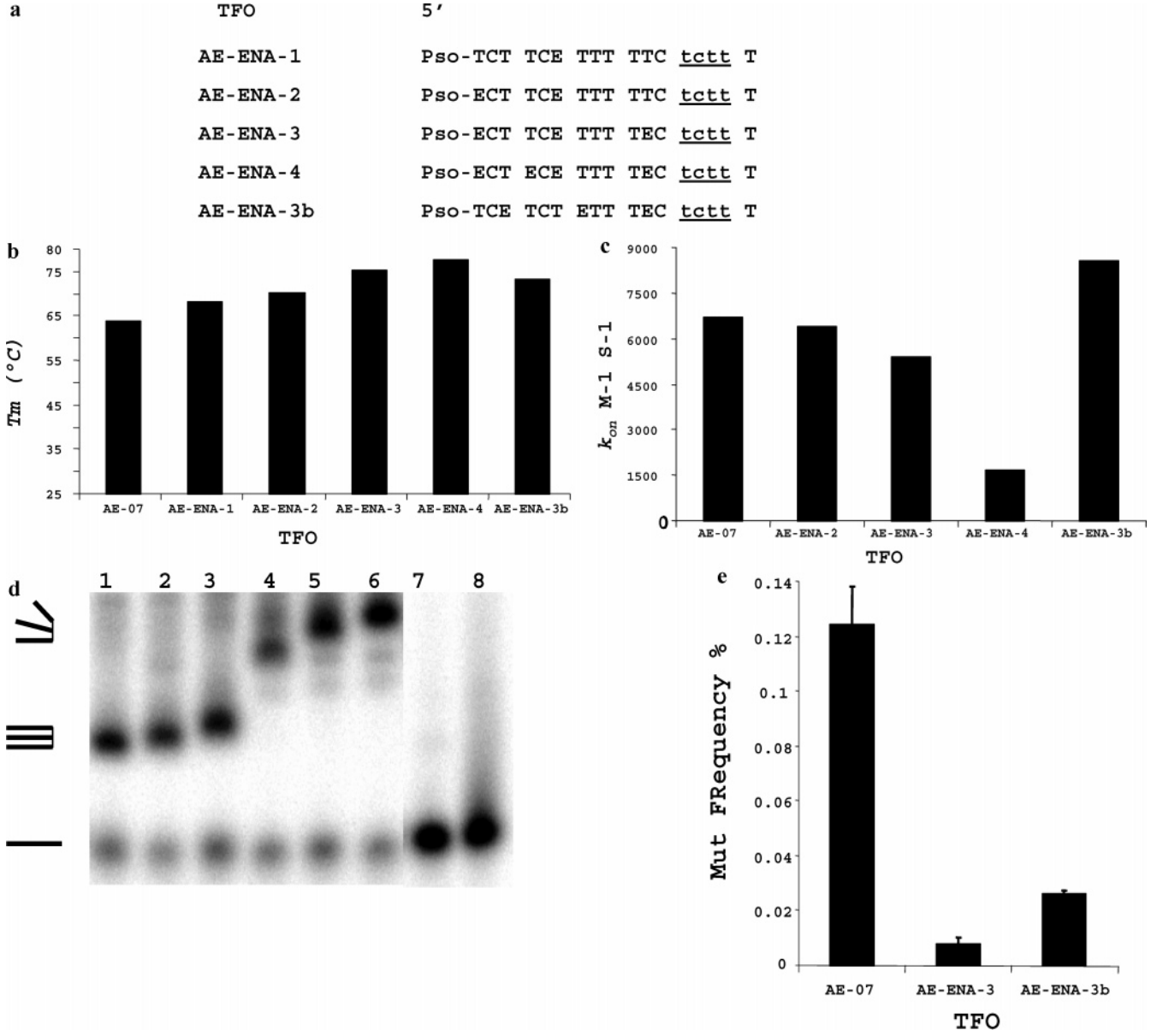


FIGURE 6: (a) Sequences and modification pattern of ENA TFOs. E indicates 2′-O,4′-C ENA thymidine. AE-ENA-1, -2, -3, and -4 contained one, two, three, and four E residues, respectively. AE-ENA-3b contained the same number of ENA monomers as AE-ENA-3; however, the distribution was different. All TFOs contained psoralen at the 5′ end. (b) Thermal stability analysis of triplexes formed by AE-ENA TFOs. (c) Relative association rate vs ENA content. (d) Electrophoretic mobility of cross-linked triplexes on a 12% polyacrylamide denaturing gel. Lanes: 1, AE-ENA-4 + duplex; 2, AE-ENA-3b + duplex; 3, AE-ENA-3 + duplex; 4, AE-ENA-2 + duplex; 5, AE-ENA-1 + duplex; 6, AE-07 + duplex; 7, duplex alone; 8, duplex purine strand. Lanes 1−6: The triplexes were UVA treated for 5 min. Extraneous lanes were removed from the gel profile. (e) Bioactivity of AE-ENA TFOs measured in the *HPRT* mutation assay.

triplexes formed by the bioinactive AE-BNA/LNA-3 and AE-ENA-3b TFOs on the G•C target were actually greater than the thermal stability of the triplex formed by the active AE-07 on the wild-type target (74.5 and 77 °C vs 66 °C).

*Triplex Formation in the Presence of Competitor Genomic DNA.* An implication of the increased affinity for nonspecific target sequences by the more extensively modified TFOs is that triplex formation on the specific target would be reduced in the presence of an excess of genomic DNA acting as a competitor. This would mimic the situation in the nucleus following introduction of the TFO. Accordingly, we incubated the AE-07 and AE-ENA-3b with a trace amount of labeled target duplex in the presence of increasing amounts of purified DNA extracted from CHO cells. The AE-ENA-3b oligonucleotide was chosen as a representative of the extensively modified, but biologically inactive TFO group. After the incubation period the samples were electrophoresed on neutral acrylamide gels to assess the extent of triplex formation (Figure 8). The gel pattern indicated virtually complete triplex formation when AE-07 was incubated with the highest amount of genomic DNA (450000-fold excess of moles of phosphate relative to the specific target oligonucleotide). However, in the presence of the highest amount of genomic competitor, triplex formation by AE-ENA-3b was reduced by 60%. Thus the data clearly indicated that triplex formation by AE-ENA-3b was much more sensitive to the presence of the genomic DNA than AE-07.

## DISCUSSION

In our previous work we demonstrated the critical contribution of appropriate sugar modification toward TFO

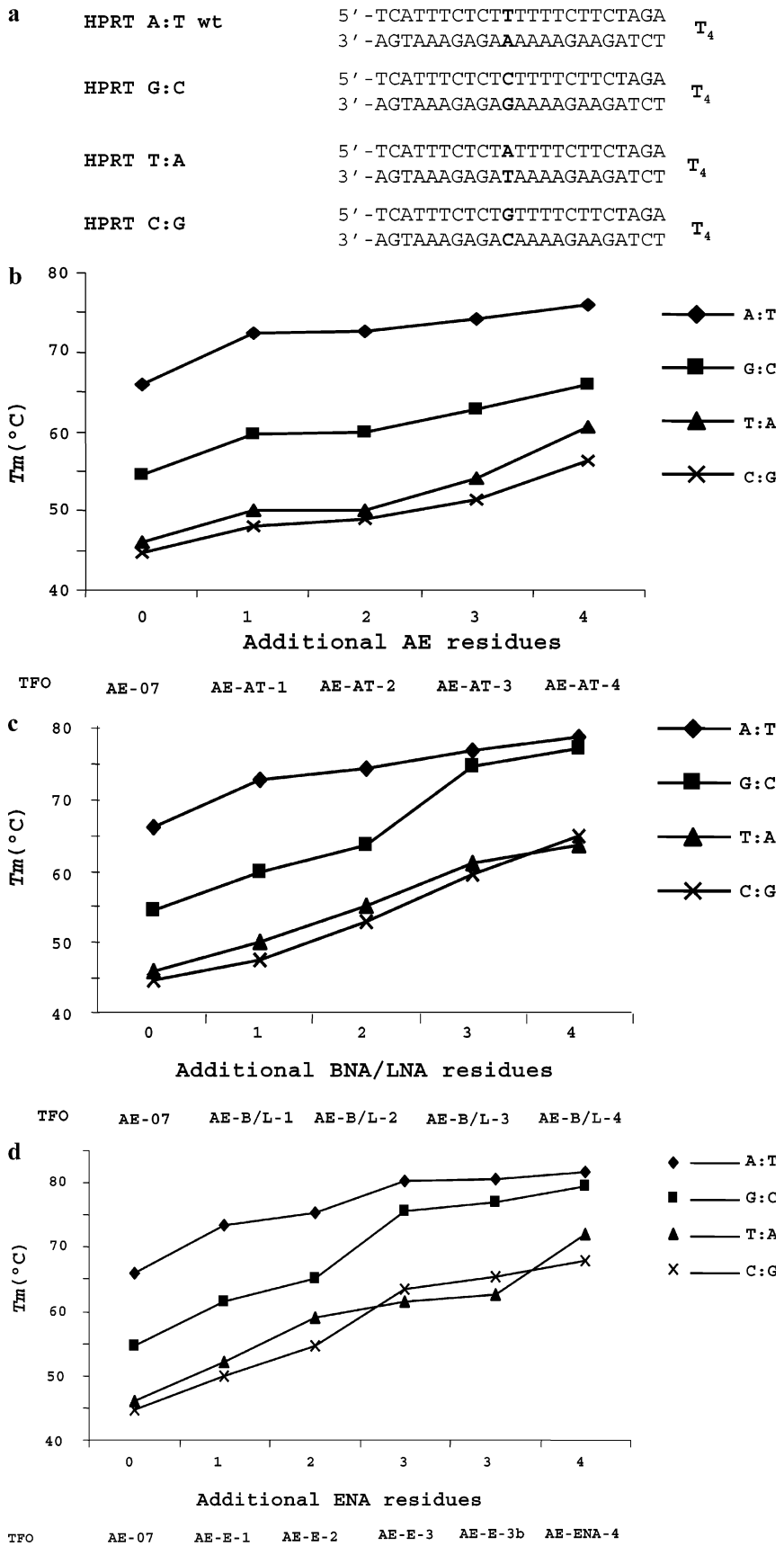


FIGURE 7: (a) Sequences of 50-mer hairpin hamster HPRT target (wt) and variants. Note the variable position in bold font. (b−d) Thermal stability of triplexes formed on the hairpin targets by (b) AE-AT TFOs, (c) AE-BNA/LNA TFOs, and (d) AE-ENA TFOs.

bioactivity (*23*, *31*). In particular, we found that TFOs with a cluster of three to four 2′-AE residues were active. These displayed association kinetics disproportionately faster than inactive TFOs with fewer 2′-AE substitutions. We concluded that the rate of association was an important parameter of bioactivity. Consequently, in our effort to further improve

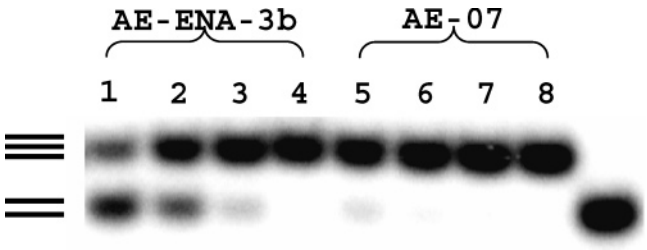


FIGURE 8: Triplex formation by AE-07 and AE-ENA-3b in the presence of genomic DNA. The $^{32}$P-labeled target duplex was incubated with the TFOs as indicated in the presence of increasing amounts of purified genomic DNA isolated from CHO cells. The samples were electrophoresed on a neutral acrylamide gel. The positions of the duplex and triplex are diagrammed. Lanes: 1 and 5, 7.5 $\mu$g of genomic DNA (450000-fold excess moles of phosphate relative to the labeled duplex); 2 and 6, 5.5 $\mu$g of genomic DNA (330000-fold excess); 3 and 7, 210000-fold excess; 4 and 8, no genomic DNA.

TFO activity, we were careful to preserve the four contiguous 2′-AE residues and to identify TFOs, with additional modifications, that maintained or enhanced $k_{ON}$ values. At the same time we wanted to modify the TFOs such that triplex stability would be enhanced, in an effort to counter the instability of triplexes in the nuclear environment of living cells (*38*). The substitution strategies described here produced TFOs that met these goals.

Two features of the additionally modified oligonucleotides merit comment.

The first is that when the extra modifications made an improvement in association rate, it was only marginally greater than that of AE-07, regardless of the modification. Apparently, the patch of four 2′-AE residues makes the primary contribution to association rate. The results of our experiments indicate that a different approach will be required to further improve the association rate. Perhaps a cluster of doubly charged residues such as the 2′-aminoethoxy-5-propargylamino-U described by Brown, Fox, and colleagues would be useful (*39*).

The second is the increased, in some cases remarkable, stability of the triplexes formed by the extensively modified TFOs. This was demonstrated by thermal stability analyses in which the TFOs with the most extensive AE, BNA/LNA, or ENA substitutions showed $T_m$ values in the range of 75−80 °C at pH 7.0. In other experiments we characterized a TFO that contained six ENA residues and formed triplexes whose $T_m$ value was greater than 90 °C. The psoralen-linked triplexes formed by these TFOs appeared to resist denaturation when examined by electrophoresis in a gel containing 7 M urea. These TFOs might be effective for in vitro applications, as probes, for triplex affinity capture, or for structural analyses (*40*, *41*).

In light of the improvements in the biochemistry and biophysical measures of TFO performance, why did the additionally modified TFOs uniformly fail in the bioassay? The similar reduction in bioactivity displayed by the members of each TFO series argues against a modification-specific explanation (too much positive charge, aggregation, etc.). Nor do we think it reflects a failure of the bioassay to faithfully report triplex formation by the new TFOs. The assay is based on the measurement of deletion mutations resulting from the targeted psoralen cross-links. We considered the possibility that the TFOs had actually formed triplexes in vivo, but the extraordinary properties of those triplexes blocked deletion formation. However, we found no evidence for the base substitutions following TFO treatment. Furthermore, we analyzed treated cells for direct biochemical evidence of targeted cross-links, as shown in previous work (*30*), but again found no evidence for their formation (not shown). Consequently, we concluded that the failure to observe TFO activity in the *HPRT* knockout assay reflected a failure of the new pso-TFOs to bind the target sequence in living cells, in marked contrast to their activity in vitro.

Although there are multiple explanations for this observation, at this time we suggest that the simplest lies in the enhanced affinity of the further substituted TFOs for nonspecific targets, as shown in Figure 7. The $T_m$ values for the more extensively modified TFOs against the nonspecific target were equivalent to that of AE-07 against the specific target. Our experiment measured stability on only one set of mismatched target sequences. Obviously, it would be impractical to determine the stability of triplexes formed on all possible mismatched targets. However, it seems reasonable to conclude that the extensively modified TFOs would form triplexes on many nonspecific sequences in the genome. We suggest that it is likely that these triplexes would be sufficiently stable such that their formation would reduce the available TFO concentration below a level required for measurable activity in the targeted knockout assay (*32*). This interpretation is consistent with the results of the competition experiment described in Figure 8. The performance of the AE-AT TFOs, which formed the least stable triplexes on the variant targets and had the greatest residual activity in the bioassay, is also consistent with this conclusion.

The results presented here are a direct test of the hypothesis that is implicit in much triplex research: that improvement of the biophysical and biochemical parameters of TFO activity will be accompanied by increased biological activity. Our results argue that this assumption, at least in its simplest form, is incorrect. If our suggestion regarding the increased affinity for nonspecific targets has value, then improvements in TFOs that are accompanied by an increased affinity for nonspecific genomic targets will actually reduce bioactivity against the specific target. This interpretation implies a sufficiently high number of nonspecific genomic targets such that they act as a sink with the potential to lower the effective concentration of the TFO in the nucleus. Thus further optimization of TFO biological activity will require synthesis of oligonucleotides with the highest association rate and affinity for intended targets and lowest for nonspecific sequences.

Although our efforts to improve the biological activity of the TFOs were not successful, we think it likely that improvements are possible. However, on the basis of this and a previous study (*42*), we have concluded that additional sugar modification is unlikely to be effective. It should be noted that the contribution of the sugar analogues is inherently nonselective with respect to sequence. Perhaps a more productive route would be the development of base analogues designed to enhance stability and association rate without increasing affinity for nonspecific targets.

## REFERENCES


1. Felsenfeld, G., Davies, D. R., and Rich, A. (1957) Formation of a three stranded polynucleotide molecule, *J. Am. Chem. Soc. 79*, 2023−2024.
2. Frank-Kamenetskii, M. D., and Mirkin, S. M. (1995) Triplex DNA structures, *Annu. Rev. Biochem. 64*, 65−95.
3. Fossella, J. A., Kim, Y. J., Shih, H., Richards, E. G., and Fresco, J. R. (1993) Relative specificities in binding of Watson-Crick base pairs by third strand residues in a DNA pyrimidine triplex motif, *Nucleic Acids Res. 21*, 4511−4515.
4. Thuong, N. T., and Helene, C. (1993) Sequence specific recognition and modification of double helical DNA by oligonucleotides, *Angew. Chem., Intl. Ed. Engl. 32*, 666−690.
5. Plum, G. E., Park, Y. W., Singleton, S. F., Dervan, P. B., and Breslauer, K. J. (1990) Thermodynamic characterization of the stability and the melting behavior of a DNA triplex: a spectroscopic and calorimetric study, *Proc. Natl. Acad. Sci. U.S.A. 87*, 9436−9440.
6. Helene, C. (1991) The anti-gene strategy: control of gene expression by triplex-forming-oligonucleotides, *Anticancer Drug Des. 6*, 569−584.
7. Chubb, J. M., and Hogan, M. E. (1992) Human therapeutics based on triple helix technology, *Trends Biotechnol. 10*, 132−136.
8. Vasquez, K. M., and Wilson, J. H. (1998) Triplex-directed modification of genes and gene activity, *Trends Biochem. Sci. 23*, 4−9.
9. Maher, L. J., III (1996) Prospects for the therapeutic use of antigene oligonucleotides, *Cancer Invest. 14*, 66−82.
10. Lee, J. S., Woodsworth, M. L., Latimer, L. J., and Morgan, A. R. (1984) Poly(pyrimidine)·poly(purine) synthetic DNAs containing 5-methylcytosine form stable triplexes at neutral pH, *Nucleic Acids Res. 12*, 6603−6614.
11. Roberts, R. W., and Crothers, D. M. (1992) Stability and properties of double and triple helices: dramatic effects of RNA or DNA backbone composition, *Science 258*, 1463−1466.
12. Escude, C., Sun, J. S., Rougee, M., Garestier, T., and Helene, C. (1992) Stable triple helices are formed upon binding of RNA oligonucleotides and their 2′-O-methyl derivatives to double-helical DNA, *C.R. Acad. Sci. III 315*, 521−525.
13. Shimizu, M., Konishi, A., Shimada, Y., Inoue, H., and Ohtsuka, E. (1992) Oligo(2′-O-methyl)ribonucleotides. Effective probes for duplex DNA, *FEBS Lett. 302*, 155−158.
14. Asensio, J. L., Carr, R., Brown, T., and Lane, A. N. (1999) Conformational and thermodynamic properties of parallel intramolecular triple helixes containing a DNA, RNA, or 2′-OMeDNA third strand, *J. Am. Chem. Soc. 121*, 11063−11070.
15. Cuenoud, B., Casset, F., Husken, D., Natt, F., Wolf, R. M., Altmann, K. H., Martin, P., and Moser, H. E. (1998) Dual recognition of double stranded DNA by 2′-aminoethoxy-modified oligonucleotides, *Angew. Chem., Intl. Ed. Engl. 37*, 1288−1291.
16. Carlomagno, T., Blommers, M. J., Meiler, J., Cuenoud, B., and Griesinger, C. (2001) Determination of aliphatic side-chain conformation using cross-correlated relaxation: application to an extraordinarily stable 2′- aminoethoxy-modified oligonucleotide triplex, *J. Am. Chem Soc. 123*, 7364−7370.
17. Osborne, S. D., Powers, V. E., Rusling, D. A., Lack, O., Fox, K. R., and Brown, T. (2004) Selectivity and affinity of triplex-forming oligonucleotides containing 2′-aminoethoxy-5-(3-aminoprop-1-ynyl)uridine for recognizing AT base pairs in duplex DNA, *Nucleic Acids Res. 32*, 4439−4447.
18. Obika, S., Uneda, T., Sugimoto, T., Nanbu, D., Minami, T., Doi, T., and Imanishi, T. (2001) 2′-O,4′-C-Methylene bridged nucleic acid (2′,4′-BNA): synthesis and triplex-forming properties, *Bioorg. Med. Chem 9*, 1001−1011.
19. Torigoe, H., Hari, Y., Sekiguchi, M., Obika, S., and Imanishi, T. (2001) 2′-O,4′-C-methylene bridged nucleic acid modification promotes pyrimidine motif triplex DNA formation at physiological pH: thermodynamic and kinetic studies, *J. Biol. Chem. 276*, 2354−2360.
20. Brunet, E., Alberti, P., Perrouault, L., Babu, R., Wengel, J., and Giovannangeli, C. (2005) Exploring cellular activity of locked nucleic acid-modified triplex-forming oligonucleotides and defining its molecular basis, *J. Biol. Chem. 280*, 20076−20085.
21. Koizumi, M., Morita, K., Daigo, M., Tsutsumi, S., Abe, K., Obika, S., and Imanishi, T. (2003) Triplex formation with 2′-O,4′-C-ethylene-bridged nucleic acids (ENA) having C3′-endo conformation at physiological pH, *Nucleic Acids Res. 31*, 3267−3273.
22. Majumdar, A., Khorlin, A., Dyatkina, N., Lin, F. L., Powell, J., Liu, J., Fei, Z., Khripine, Y., Watanabe, K. A., George, J., Glazer, P. M., and Seidman, M. M. (1998) Targeted gene knockout mediated by triple helix forming oligonucleotides, *Nat. Genet. 20*, 212−214.
23. Puri, N., Majumdar, A., Cuenoud, B., Miller, P. S., and Seidman, M. M. (2004) Importance of clustered 2′-O-(2-aminoethyl) residues for the gene targeting activity of triple helix-forming oligonucleotides, *Biochemistry 43*, 1343−1351.
24. Blommers, M. J., Natt, F., Jahnke, W., and Cuenoud, B. (1998) Dual recognition of double-stranded DNA by 2′-aminoethoxy-modified oligonucleotides: the solution structure of an intramolecular triplex obtained by NMR spectroscopy, *Biochemistry 37*, 17714−17725.
25. Morita, K., Yamate, K., Kurakata, S., Watanabe, K., Imanishi, T., and Koizumi, M. (2003) 2′-O,4′-C-ethylene-bridged nucleic acid (ENA) for effective antisense formation, *Nucleosides, Nucleotides, Nucleic Acids 22*, 1619−1621.
26. Puri, N., Majumdar, A., Cuenoud, B., Natt, F., Martin, P., Boyd, A., Miller, P. S., and Seidman, M. M. (2001) Targeted gene knockout by 2′-O-aminoethyl modified triplex forming oligonucleotides, *J. Biol. Chem. 276*, 28991−28998.
27. Xodo, L. E. (1995) Kinetic analysis of triple-helix formation by pyrimidine oligodeoxynucleotides and duplex DNA, *Eur. J. Biochem. 228*, 918−926.
28. Arya, D. P., Coffee, R. L., Jr., and Charles, I. (2001) Neomycin-induced hybrid triplex formation, *J. Am. Chem Soc. 123*, 11093−11094.
29. Orren, D. K., Petersen, L. N., and Bohr, V. A. (1997) Persistent DNA damage inhibits S-phase and G2 progression, and results in apoptosis, *Mol. Biol. Cell 8*, 1129−1142.
30. Majumdar, A., Puri, N., Cuenoud, B., Natt, F., Martin, P., Khorlin, A., Dyatkina, N., George, A. J., Miller, P. S., and Seidman, M. M. (2003) Cell cycle modulation of gene targeting by a triple helix-forming oligonucleotide, *J. Biol. Chem. 278*, 11072−11077.
31. Puri, N., Majumdar, A., Cuenoud, B., Natt, F., Martin, P., Boyd, A., Miller, P. S., and Seidman, M. M. (2002) Minimum number of 2′-O-(2-aminoethyl) residues required for gene knockout activity by triple helix forming oligonucleotides, *Biochemistry 41*, 7716−7724.
32. Richards, S., Liu, S. T., Majumdar, A., Liu, J. L., Nairn, R. S., Bernier, M., Maher, V., and Seidman, M. M. (2005) Triplex targeted genomic crosslinks enter separable deletion and base substitution pathways, *Nucleic Acids Res. 33*, 5382−5393.
33. Vester, B., and Wengel, J. (2004) LNA (locked nucleic acid): high-affinity targeting of complementary RNA and DNA, *Biochemistry 43*, 13233−13241.
34. Sun, B. W., Babu, B. R., Sorensen, M. D., Zakrzewska, K., Wengel, J., and Sun, J. S. (2004) Sequence and pH effects of LNA-containing triple helix-forming oligonucleotides: physical chemistry, biochemistry, and modeling studies, *Biochemistry 43*, 4160−4169.
35. Brunet, E., Corgnali, M., Cannata, F., Perrouault, L., and Giovannangeli, C. (2006) Targeting chromosomal sites with locked nucleic acid-modified triplex-forming oligonucleotides: study of efficiency dependence on DNA nuclear environment, *Nucleic Acids Res. 34*, 4546−4553.
36. Shahid, K. A., Majumdar, A., Alam, R., Liu, S. T., Kuan, J. Y., Sui, X., Cuenoud, B., Glazer, P. M., Miller, P. S., and Seidman, M. M. (2006) Targeted cross-linking of the human beta-globin gene in living cells mediated by a triple helix forming oligonucleotide, *Biochemistry 45*, 1970−1978.
37. Morita, K., Takagi, M., Hasegawa, C., Kaneko, M., Tsutsumi, S., Sone, J., Ishikawa, T., Imanishi, T., and Koizumi, M. (2003) Synthesis and properties of 2′-O,4′-C-ethylene-bridged nucleic acids (ENA) as effective antisense oligonucleotides, *Bioorg. Med. Chem. 11*, 2211−2226.
38. Lin, F. L., Majumdar, A., Klotz, L. C., Reszka, A. P., Neidle, S., and Seidman, M. M. (2000) Stability of DNA triplexes on shuttle vector plasmids in the replication pool in mammalian cells, *J. Biol. Chem. 275*, 39117−39124.
39. Sollogoub, M., Darby, R. A., Cuenoud, B., Brown, T., and Fox, K. R. (2002) Stable DNA triple helix formation using oligonucleotides containing 2′-aminoethoxy-5-propargylamino-U, *Biochemistry 41*, 7224−7231.
40. Johnson, M. D., III, and Fresco, J. R. (1999) Third-strand in situ hybridization (TISH) to non-denatured metaphase spreads and interphase nuclei, *Chromosoma 108*, 181−189.

41. Nadal, A., Coll, A., Avino, A., Esteve, T., Eritja, R., and Pla, M. (2006) Efficient sequence-specific purification of Listeria innocua mRNA species by triplex affinity capture with parallel tail-clamps, *ChemBioChem 7*, 1039−1047.
42. Kundu, M., Nagatsugi, F., Majumdar, A., Miller, P. S., and Seidman, M. M. (2003) Enhancement and inhibition by 2′-O-hydroxyethyl residues of gene targeting mediated by triple helix forming oligonucleotides, *Nucleosides, Nucleotides, Nucleic Acids 22*, 1927−1938.

BI7003153